Optimization of Technological Parameters when Plasma Nitriding the Gear Working Surface

Bui Thanh Danh

Faculty of Mechanical Engineering, University of Transport and Communications, Vietnam
danhdaiduong@utc.edu.vn

Le Hong Ky

Vinh Long University of Technology Education, Vietnam
kylh@vlute.edu.vn (corresponding author)

ABSTRACT

This paper presents the results of optimizing the technological parameters when plasma nitriding the gear working surface. 27 experiments were carried out on an H4580 Eltrolab instrument to obtain a working surface hardness database table, and the Minitab statistical software was used to process the experimental results. A regression equation was identified to analyze the influence of temperature, time, and gas permeation concentration on the hardness of the working surface. An analysis of variance (ANOVA) showed that all these nitriding parameters influence the regression equation. The results showed that the permeation temperature *TL* has the greatest influence on the hardness, while the permeation time *h* and the first gas permeation concentration G1 had less influence. An optimal set of technological parameters was established, where the permeation temperature was *TL*=550°C, permeation time was *h*=8h, and the first gas permeation concentration was *G*1=4l/h. Experiments were carried out using this set of optimal parameters to evaluate the microstructure and the depth of the hardening layer of the part surface. Finally, this study presented the whole process for the permeation and plasma nitriding of 18ХГТ steel.

Keywords-permeation temperature; permeation time; gas permeation concentration; working surface hardness; plasma nitriding; regression

I. INTRODUCTION

Plasma nitriding is widely used in steel machine parts [1-2], as it can control the white layer making it very suitable for creating products with high-quality requirements [3-5]. The permeation process is carried out at low pressure in a vacuum furnace with a mixture of H_2, N_2, CH_4, and Ar gases [1, 3-4, 6-7]. These gases are ionized under high voltage, creating a plasma. Nitrogen ions are accelerated during the collision of the plasma with the sample. This ion bombardment heats, cleans, and forms a hard layer with good wear resistance, increasing fatigue strength [7]. In recent years, many studies have been conducted on the nitriding process model, but it is generally not enough to predict the influence of the parameters on the quality of the permeable layer [3-5, 9-13].

In [9], Wagner's generalized common model was used to analyze the permeable layer formation and use it in plasma nitriding experiments. The parabolic curve in the proposed predictive models shows the increase in nitrogen content in the permeable layer and the diffusion area in plasma nitriding [5, 9]. In [14], a numerical simulation model was presented for the nitride layer growth and nitrogen distribution in the ε, γ', and α

phases during plasma nitriding of low-carbon steel. The results showed that the nitride layers consist of ε, γ', and α phases and that the thickness of these phases follows a parabolic pattern. In [9], a numerical model of nitrogen diffusion in low-carbon steel was presented, showing that diffusion depended on nitrogen concentration and that the thickness of the permeable layers was the square root of the nitriding time at 843°K (570°C). In [15], a nitriding process model for low-carbon steel was investigated, performing gas nitriding using NH_3-H_2 gas permeation. A simple model was designed to predict the thickness of the nitride layers in pure iron, built using a kinetic model derived from Fick's second law. Several studies attempted to predict and evaluate the distribution of nitrogen concentrations and nitride compounds formed during pure iron nitriding and the depth of the nitrogen diffusion area after plasma nitriding [3, 8, 16]. As the plasma power increases, the maximum adhesion values change, reaching 80MPa when the plasma power approaches 80kW [11]. In [12], the influence of plasma nitriding technology parameters on the deformation of hypoid gears was investigated, using blue light technology with a non-contact measuring device to determine the deformation after plasma nitriding.

There is a lack of studies on plasma nitriding for parts made of 18ХГТ alloy steel (equivalent to SAE 5120) [2, 6, 12, 17]. This study used an ELTROPUL permeation furnace with a pre-made plasma pulse source with stable plasma flow in all cases and easily penetrating details with complex geometries. Along with mathematical statistics tools and Minitab software, methods such as EDAS, MARCOS, TOPSIS, MOORA, and PIV [11-13, 18-25] were used to design and process the experimental data of this study.

II. EXPERIMENTAL PROCESS

The plasma nitriding sample consists of passive hypoid gear teeth, machined from alloy steel 18ХГТ according to the Russian standards (equivalent to SAE 5120) [2, 6, 17], having a chemical composition of (%): C: 0.17 – 0.23; Si: 0.17 – 0.37; Mn: 0.8 – 1.1; P: < 0.035; S: < 0.035; Cr: 1 – 1.3; Ni: < 0.3; Ti: 0.03 – 0.09; Cu: < 0.3; N: < 0.008) [2]. The gear was hardened to achieve a hardness ranging from 34-36HRC, equivalent to 336-354HV of the Vickers hardness measurement, and then each tooth was cut apart by the wire cutting method, in order from 1 to 27, as shown in Figure 1.

(a)

(b)

Fig. 1.   Sample preparation: (a) Hypoid gear pairs after machining, (b) plasma nitriding samples cut from hypoid gears.

According to the JIS Z 2244-2009 standard, a control sample of the same material was included in addition to the experimental sample when conducting each experiment. An H4580 Eltrolab was used to perform programmable plasma nitriding, and the following parameters could be set when programming [5]: number of hours executed in each step of the program h, number of minutes executed in each step of the program m, pressure P (in pascals), permeation temperature TL ($^\circ$C), temperature rise rate of the furnace over time TG ($^\circ$C/min), furnace wall temperature TW ($^\circ$C), temperature rise rate of the furnace wall over time WG ($^\circ$C/min), voltage V (V), pulse duration PD (μs), number of pulse repetitions PR (μs), gas flow 1 $G1$ (l/h), gas flow 2 $G2$ (l/h), gas flow 3 $G3$ (ml/h), and gas flow 4 $G4$ (l/h).

The permeation process with samples of the same material and size changes little the permeation temperature TL, so the voltage V and pressure P were fixed [1, 11, 26]. The temperature rise rate of the part over time TG, furnace wall temperature TW, and temperature rise rate of the furnace wall

over time WG depend on permeation temperature TL and permeation time h. Gas permeation flows $G1$, $G2$, $G3$, and $G4$ are proportional to each other [26]. According to the requirements for selecting input factors, the experimental variables of temperature TL, permeation time h, and first gas permeation concentration $G1$ were selected. The remaining factors remained unchanged. A total of 27 experiments were planned and the program to control the permeation process was set on the H4580 Eltrolab software. As the depth of the plasma nitriding layer on the surface of the experimental sample was very thin (μm), the microscopic hardness was tested using the Vickers hardness measurement method (HV) according to the JIS Z 2244-2009 standard with an FM-700e. Table I shows the experimental results.

TABLE I.   EXPERIMENTAL RESULTS

Trial	Permeation time h (h)	Permeation temperature TL ($^\circ$C)	Gas flow 1 $G1$ (l/h)	Hardness, H (HV)
1	4	510	4	632.0
2	4	510	6	644.2
3	4	510	8	654.1
4	4	530	4	670.7
5	4	530	6	676.2
6	4	530	8	678.8
7	4	550	4	699.9
8	4	550	6	700.4
9	4	550	8	694.2
10	6	510	4	638.1
11	6	510	6	641.3
12	6	510	8	653.5
13	6	530	4	670.6
14	6	530	6	677.9
15	6	530	8	676.4
16	6	550	4	703.1
17	6	550	6	701.5
18	6	550	8	693.9
19	8	510	4	652.7
20	8	510	6	652.7
21	8	510	8	659.7
22	8	530	4	684.8
23	8	530	6	681.4
24	8	530	8	684.3
25	8	550	4	717.0
26	8	550	6	706.1
27	8	550	8	701.9

III. RESULTS AND DISCUSSIONS

An analysis of variance (ANOVA) was carried out on the regression equation results, to remove the parameters that do not affect them [11, 14, 16-24]. The regression equation for hardness H can be written as follows:

$$H = -2726 - 6.44\,h + 10.52\,TL + 87.17\,G + 1.090\,h^2 - 0.00776\,TL^2 - 0.690\,h \times G1 - 0.1552\,TL \times G1 \qquad (1)$$

Figure 2 and regression show that TL has the greatest influence on hardness, while h and $G1$ have less. In Figure 2, the effect of h is parabolic, starting from a level (0), reaches a minimum, and finally approaches the maximum value of 685HV in the level area (+1) of the planning. The effect of TF is almost linear, starting at 645HV and reaching a maximum value of about 700HV. The effect of $G1$ is linear, starting from

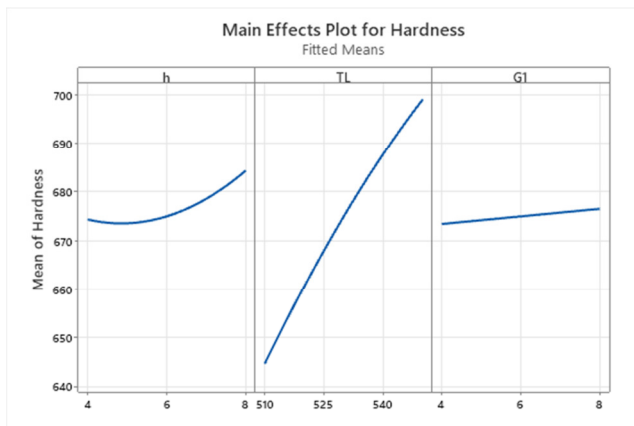the minimum value at level (-1) and reaching the maximum value at level (+1).

Fig. 2.   The influence of parameters on hardness.

Figure 3 shows a plot of the standardized effects of parameters on the hardness of the working surface. *TL* has the greatest influence on hardness, followed by *h*, while *G1* has the lowest influence. The interaction between *TL*, *G*1, and *h* greatly affects the hardness of the surface. These results are consistent with the theoretical basis of the first and second Fick laws since the temperature is the main factor that strongly influences the coefficients and diffusion. Maximal optimization was carried out with the following boundary conditions:

$$\max Hardness : \begin{cases} 4 \le h \le 8 \\ 510 \le TL \le 550 \\ 4 \le G1 \le 8 \end{cases}$$
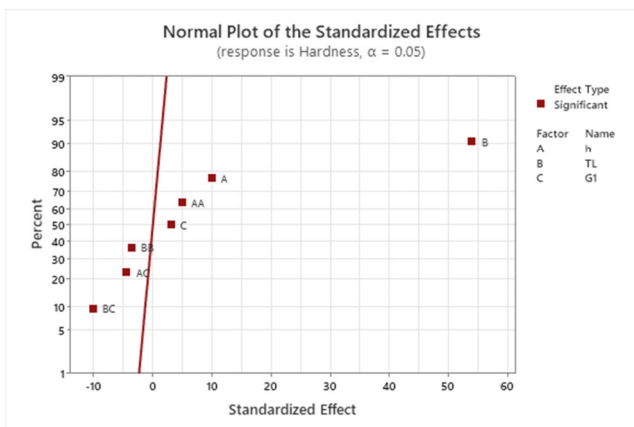
providing the results shown in Table II.

Fig. 3.   Standardized effects of variables for hardness.

TABLE II.   OPTIMIZATION RESULTS USING BOUNDARY CONDITIONS

Solution	h	TL	G1	Hardness fit
1	8	550	4	715.876

The maximum optimization value of stiffness in the planning area was 715.876 at *h*=8h, *TL*=550°C, and G1=4l/h. Experiments were carried out using the optimal set of parameters to evaluate the microstructure and hardening layer depth of the detailed surface. Figure 4 shows the optimization analysis chart.

Fig. 4.   Optimization analysis chart.

Figure 5 shows the microstructure image, indicating that the surface of the test sample corresponds to the materials of the part with a clear, permeable layer. The ε and γ' phases are the white layers that can be seen when etching and taking photos through a microscope. The microscopic organization includes carbides and nitrites distributed in ferrite.
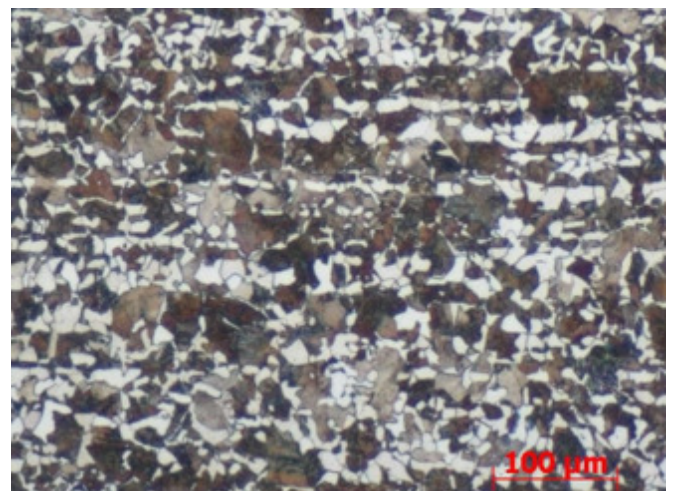

Fig. 5.   Microstructure of the plasma nitriding layer.

Phase ε has a needle shape, as shown by the chemical composition analysis of the permeable layer, using the SEM/EDX (line-scan) method in Figure 6. The microscopic examination showed carbide and nitrite distributed in Ferrite and Perclite. The microscopic hardness to the penetration depth was measured on a cross-section through the permeable layer and at intervals. Surface hardness was high and decreased when depth increased up to 350μm, where it remained constant, corresponding to the hardness of the base metal (340HV). The %N content can be determined by the thickness of the phases ε, λ, and α and the depth of the permeable layer. Figure 8 shows the EDX analysis results, illustrating that the %N content on the surface was high (10.68%N), but the deeper into the interior, the lower it was.
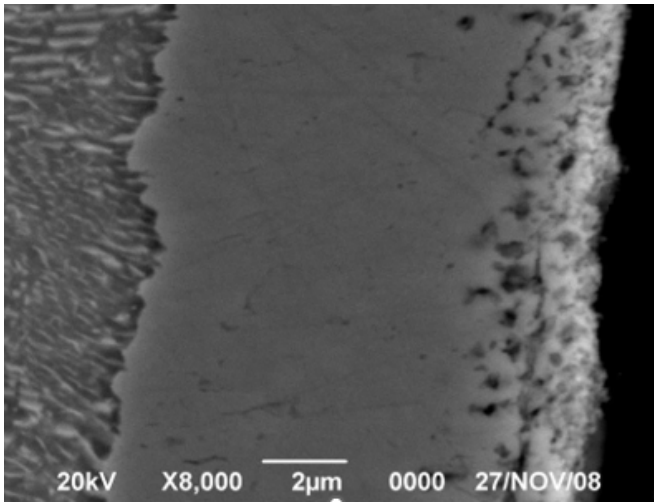
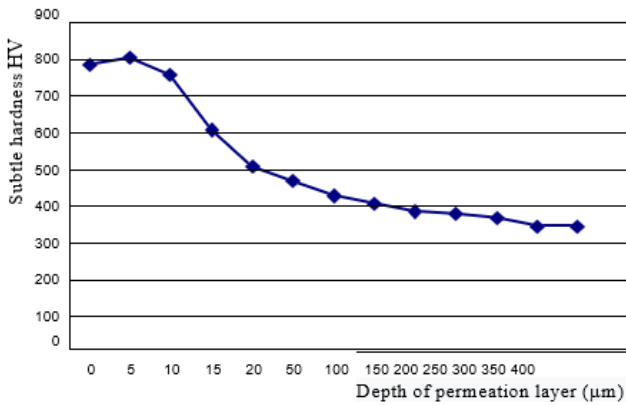Fig. 6.   SEM image (x8000).

Fig. 7.   Hardness distribution with the depth of penetration.

Figure 9 shows the EDX analysis at one location of the sample, while Figure 10 shows the nitriding process of hypoid gear pairs using the optimal parameters. Except for the optimal set of the examined parameters, the remaining parameters were fixed when conducting experiments.
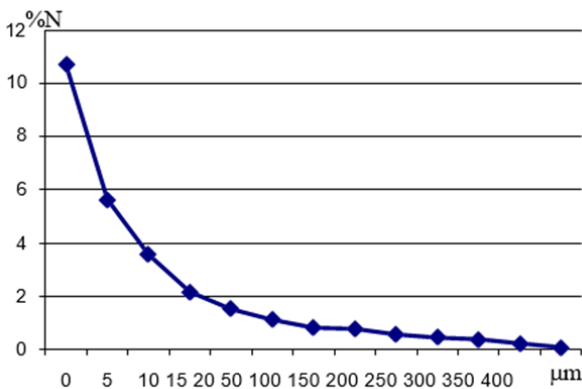

Fig. 8.   Nitrogen composition according to penetration depth.

The process of plasma nitriding can be summarized as follows:

- Clean the details to be absorbed

- Check the permeation equipment system (electrical, air conduction, cooling)

- Fix the details and put into the furnace box (make sure the details are installed tightly, do not move during the infiltration process)

- The power is closed under high voltage and low pressure to heat for the first time until it reaches approximately 250-300^{0}C. This temperature is then maintained to activate the surface. After about 2.5h, the temperature should raise at a rate of 100°C/min (second heating phase) until the permeation temperature reaches 550^{0}C. The end of the 8-hour permeation period is the auto-cooling period, as shown in Figure 10.
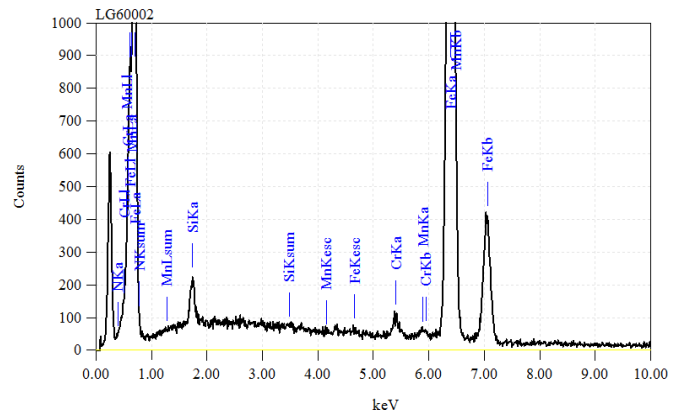
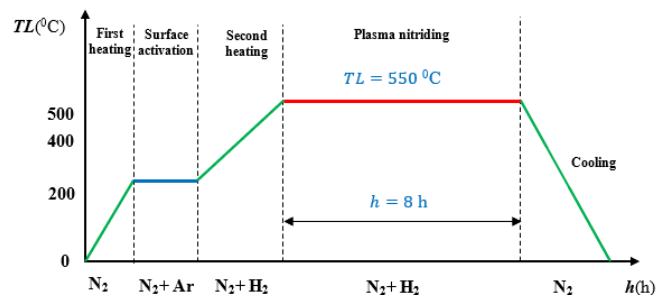

Fig. 9.   EDX analysis at one location on the sample.

Fig. 10.   Plasma nitriding technology process of hypoid gear pairs.

IV.   CONCLUSIONS

This study identified a regression equation as the basis for analyzing the influence of temperature, time, and gas concentration on the hardness of the working surface of a gear. The results of the analysis showed that the permeability temperature *TL* had the greatest influence on hardness, followed by the permeation time *h* and the gas concentration *G*1. The interaction between infiltration temperature TL, gas permeation concentration *G*1, and permeation time *h* also affects surface hardness, but to a different extent.

The results of this study were completely consistent with the theoretical basis of the first and second Fick laws. The maximum optimization value of stiffness in the planning area was 715,876, using *h*=8h, *TL*=550°C, and *G*1=4l/h. Experiments were carried out using these parameters to evaluate the microorganism and the depth of the hardening layer of the surface. The control program for the permeation process and the plasma nitriding technology process of hypoid gear pairs made of 18ХГТ steel were proposed. The proposed optimized set of technological parameters can be used when plasma nitriding various machine parts made of 18ХГТ or equivalent materials to get an optimal result.

REFERENCES

[1] D. Pye, *Practical Nitriding and Ferritic Nitrocarburizing*. Ohio, USA: ASM International, 2003.

[2] "Марочник сталей и сплавов онлайн - скачать PDF," *Metal Place*. https://metal.place/ru/wiki/18khgt/.

[3] U. Huckel and S. Strämke, "Pulsed Plasma Nitriding of Sintered Parts – Production Experiences," ELTRO GmbH, 2003.

[4] U. Huckel, "Short Description of Pulsed Plasma Nitriding," ELTRO GmbH, 2005.

[5] V. I. Dimitrov, G. Knuyt, L. M. Stals, J. D'Haen, and C. Quaeyhaegens, "Generalized Wagner's diffusion model of surface modification of materials by plasma diffusion treatment," *Applied Physics A: Materials Science & Processing*, vol. 67, no. 2, pp. 183–192, Aug. 1998, https://doi.org/10.1007/s003390050757.

[6] "ISO TR 22849 - Design recommendations for bevel gears," International Standards Organization, Geneva, Switzerland, Standard, 2011.

[7] D. Y. Chung, H. J. Kim, and H. N. Kim, "A Study on the Erosion Characteristics of the Micropulsed Plasma Nitrided Barrel of a Riffle," presented at the 19th International Symposium of Ballistics, Interlaken, Switzerland, May 2001.

[8] T. K. Hirsch, A. D. S. Rocha, F. D. Ramos, and T. R. Strohaecker, "Residual stress-affected diffusion during plasma nitriding of tool steels," *Metallurgical and Materials Transactions A*, vol. 35, no. 11, pp. 3523–3530, Nov. 2004, https://doi.org/10.1007/s11661-004-0189-2.

[9] U. Huckel, S. Strämke, and J. Cockrem, "Pulsed Plasma Nitriding of Tools," ELTRO GmbH, 2003.

[10] O. Onmus, "Microstructural and mechanical characterization of nitrogen ion implanted and plasma ion nitrided plastic injection mould steel," MSc Thesis, Izmir Institute of Technology, Izmir, Turkey, 2003.

[11] D. Vu, "Prediction of the Adhesion Strength of Coating in Plasma Spray Deposition," *Engineering, Technology & Applied Science Research*, vol. 13, no. 2, pp. 10367–10371, Apr. 2023, https://doi.org/10.48084/etasr.5673.

[12] H. K. Le, "A Study on the Influence of Plasma Nitriding Technology Parameters on the Working Surface Deformation of Hypoid Gears," *Engineering, Technology & Applied Science Research*, vol. 12, no. 6, pp. 9760–9765, Dec. 2022, https://doi.org/10.48084/etasr.5365.

[13] D. D. Trung, "Application of EDAS, MARCOS, TOPSIS, MOORA and PIV Methods for Multi-Criteria Decision Making in Milling Process," *Strojnícky časopis - Journal of Mechanical Engineering*, vol. 71, no. 2, pp. 69–84, Nov. 2021, https://doi.org/10.2478/scjme-2021-0019.

[14] M. Yan, J. Yan, and T. Bell, "Numerical simulation of nitrided layer growth and nitrogen distribution in ε-Fe2-3N, γ'-Fe4N and α-Fe during pulse plasma nitriding of pure iron," *Modelling and Simulation in Materials Science and Engineering*, vol. 8, no. 4, pp. 491–496, Jul. 2000, https://doi.org/10.1088/0965-0393/8/4/307.

[15] M. Keddam, "Surface modification of the pure iron by the pulse plasma nitriding: Application of a kinetic model," *Materials Science and Engineering: A*, vol. 462, no. 1, pp. 169–173, Jul. 2007, https://doi.org/10.1016/j.msea.2006.02.459.

[16] M. B. Karamiş, "Some effects of the plasma nitriding process on layer properties," *Thin Solid Films*, vol. 217, no. 1, pp. 38–47, Sep. 1992, https://doi.org/10.1016/0040-6090(92)90603-9.

[17] "Worldwide equivalent grades SAE5120 (AISI, ASTM, UNS)." http://www.steelnumber.com/en/equivalent_steel_iron_eu.php?zname_id=11848.

[18] V. C. Nguyen, T. D. Nguyen, and D. H. Tien, "Cutting Parameter Optimization in Finishing Milling of Ti-6Al-4V Titanium Alloy under MQL Condition using TOPSIS and ANOVA Analysis," *Engineering, Technology & Applied Science Research*, vol. 11, no. 1, pp. 6775–6780, Feb. 2021, https://doi.org/10.48084/etasr.4015.

[19] D. D. Trung, "Effect of Cutting Parameters on the Surface Roughness and Roundness Error When Turning the Interrupted Surface of 40X Steel Using HSS-TiN Insert," *Applied Engineering Letters : Journal of Engineering and Applied Sciences*, vol. 7, no. 1, pp. 1–9, 2022, https://doi.org/10.18485/aeletters.2022.7.1.1.

[20] D. D. Trung, "Influence of Cutting Parameters on Surface Roughness in Grinding of 65G Steel," *Tribology in Industry*, vol. 43, no. 1, pp. 167–176, Mar. 2021, https://doi.org/10.24874/ti.1009.11.20.01.

[21] D. D. Trung, N.-T. Nguyen, and D. V. Duc, "Study on Multi-Objective Optimization of the Turning Process of EN 10503 Steel by Combination of Taguchi Method and Moora Technique," *EUREKA: Physics and Engineering*, vol. 2, pp. 52–65, Mar. 2021, https://doi.org/10.21303/2461-4262.2020.001414.

[22] D. D. Trung, "Effect of Cutting Parameters on the Surface Roughness and Roundness Error When Turning the Interrupted Surface of 40X Steel Using HSS-TiN Insert," *Applied Engineering Letters : Journal of Engineering and Applied Sciences*, vol. 7, no. 1, pp. 1–9, 2022, https://doi.org/10.18485/aeletters.2022.7.1.1.

[23] D. D. Trung, "Application of TOPSIS an PIV Methods for Multi-Criteria Decision Making in Hard Turning Process," *Journal of Machine Engineering*, vol. 21, no. 4, pp. 57–71, Dec. 2021, https://doi.org/10.36897/jme/142599.

[24] D. D. Trung, "The Combination of Taguchi – Entropy – WASPAS - PIV Methods for Multi-Criteria Decision Making when External Cylindrical Grinding of 65G Steel," *Journal of Machine Engineering*, vol. 21, no. 4, pp. 90–105, Dec. 2021, https://doi.org/10.36897/jme/144260.

[25] D. D. Trung, "A combination method for multi-criteria decision making problem in turning process," *Manufacturing Review*, vol. 8, 2021, https://doi.org/10.1051/mfreview/2021024.

[26] J. C. Díaz-Guillén *et al.*, "Surface Properties of Fe4N Compounds Layer on AISI 4340 Steel Modified by Pulsed Plasma Nitriding," *Journal of Materials Science & Technology*, vol. 29, no. 3, pp. 287–290, Mar. 2013, https://doi.org/10.1016/j.jmst.2013.01.017.